

Adaptive Stylization Modulation for Domain Generalization Semantic Segmentation

Tjio Gabriel, Liu Ping, Kwoh Chee Keong and Zhou Tianyi Joey

Abstract—Obtaining sufficient labelled data for model training is impractical for most real-life applications. Therefore, we address the problem of domain generalization for semantic segmentation tasks to reduce the need to acquire and label additional data. Recent work on domain generalization increase data diversity by varying domain-variant features such as colour, style and texture in images. However, excessive stylization or even uniform stylization may reduce performance. Performance reduction is especially pronounced for pixels from minority classes, which are already more challenging to classify compared to pixels from majority classes. Therefore, we introduce a module, ASH_+ , that modulates stylization strength for each pixel depending on the pixel's semantic content. In this work, we also introduce a parameter that balances the element-wise and channel-wise proportion of stylized features with the original source domain features in the stylized source domain images. This learned parameter replaces an empirically determined global hyperparameter, allowing for more fine-grained control over the output stylized image. We conduct multiple experiments to validate the effectiveness of our proposed method. Finally, we evaluate our model on the publicly available benchmark semantic segmentation datasets (Cityscapes and SYNTHIA). Quantitative and qualitative comparisons indicate that our approach is competitive with state-of-the-art. Code is made available at <https://github.com/placeholder>.

Index Terms—Domain Generalization, Semantic Segmentation, Adaptive Data augmentation

1 INTRODUCTION

Deep learning has advanced the state-of-the-art performance in several fields, such as image classification [1], speech recognition [2] and machine translation [3]. However, this vastly improved performance requires large amounts of labelled training data, which may not be available for many real-world applications [4], [5]. The resources required for collecting sufficient real-world data and labelling the collected data pose a challenge to the adoption of deep learning techniques. This problem is further exacerbated for real-world applications [4], [5] that require expert knowledge for data labelling. For semantic segmentation tasks, labelling requires considerable effort because all the pixels in the training images must be annotated. While replacing real-world data with synthetic data significantly reduces the effort required for labeling, the domain shift [6] between the synthetic data (source domain data) and real-world images (target domain data) considerably reduces performance on the target domain data. Prior domain adaptation works [7], [8], [9], [10], [11], [12] demonstrate the effectiveness of leveraging unlabeled target domain data to minimize the performance drop caused by domain shift. However, for many real-life applications, target domain data may be unavailable because of data privacy issues and safety concerns.

- *institutional affiliations info.*

Liu Ping (corresponding author)

*Gabriel Tjio, Liu Ping and Joey Tianyi Zhou are with the Center for Frontier AI Research, A*STAR. (email:liu_ping@cfar.a-star.edu.sg, gabriel_tjio@cfar.a-star.edu.sg, joey_zhou@cfar.a-star.edu.sg)*

Kwoh Chee Keong is with the Nanyang Technological University (email:asckkwoh@ntu.edu.sg)

Domain generalization aims to mitigate the impact of domain shift when target domain data are unavailable during training. Thus far, domain generalization work can be categorized into two groups: single-source domain generalization [13], [14], [15] and multiple-source domain generalization [16]. The former approach involves training a model with a labelled source domain dataset while the latter approach uses multiple labelled source domain datasets during training. Compared to single-source domain generalization, multiple-source domain generalization is more difficult to implement for real-life applications because of the increased costs of acquiring and labelling additional domain datasets. While single-source domain generalization is more practical, its performance may be limited by the restricted variations in the single source dataset. Consequently, single-source domain generalization is usually outperformed by its multi-source domain counterpart.

Thus, most existing works [7], [13], [14] rely on hallucination-based approaches to address the limitations of single-source domain generalization. By generating additional data via label-preserving transformations on the source domain data, hallucination-based approaches [7], [13], [15] present promising solutions for single-source domain generalization. The transformations adopted in prior works typically alter the color and texture information of the source domain images while preserving the shape and structure information. The rationale behind this approach is that randomly varying these features removes the spurious correlations between these features and the ground truth labels. These spurious correlations do not generalize well to the target domain, resulting in poorer performance. Conversely, domain-invariant features such as shape and structure information are better predictors of the ground truth labels for the target domain data because they are

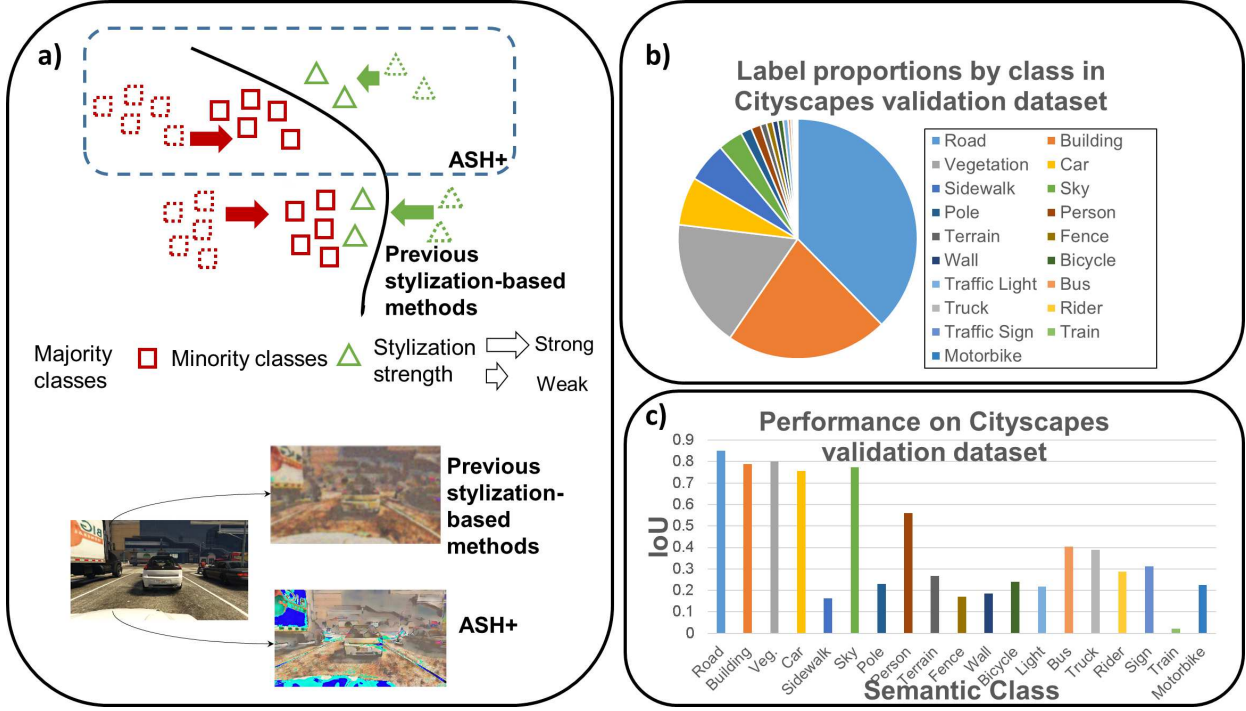


Fig. 1: Illustration of the challenges of using stylization-based methods for domain generalization. Previous methods uniformly stylize the source domain images without considering spatial or class information. In contrast, our approach conditions the stylization with the segmentation output. Uniform stylization disproportionately affects target domain performance on minority classes compared to majority classes because of the increased task difficulty associated with minority classes.

generally consistent across the source domain and target domain datasets.

Although hallucination-based approaches can improve the diversity of the training data, they still face certain limitations. As demonstrated in Figure 1a), many existing works [13], [15] apply uniform stylization to source domain images without taking into account the variations between pixels. As shown in Figure 1b and c), pixels belonging to majority classes, such as 'road', 'sky', and 'building', are relatively easier to classify due to the availability of more training examples. Secondly, the difficulty of pixel classification also varies based on its spatial location within the image. For instance, pixels located at the boundaries between different classes are generally more challenging to classify compared to pixels within a single class. Thus, applying uniform stylization to the source domain images without considering these differences may negatively impact generalization performance, particularly for minority classes.

This paper extends our earlier work [17] by introducing Adversarial Semantic Hallucination+ (ASH_+), which allows for a fine-grained control of stylization strength during training. Similar to our earlier work [17], ASH_+ leverages the semantic information of each pixel in the source domain images, which is extracted using the task segmentation model to condition the stylization strength of the source domain images. However, we significantly improve our earlier work with ASH_+ by replacing a predefined hyperparameter.

Specifically, in ASH [17], a global predefined hyperparameter was used to control the stylization strength. In this work, however, we suggest that a global hyperparameter does not adequately account for the spatial and class-wise differences that affect classification difficulty. Therefore, for ASH_+ , we take into account the spatial and channel-wise variations of the source and perturbed style features in the stylized images. Our design allows for greater diversity in the generated stylized image, which boosts the trained model generalization ability. To demonstrate the efficacy of our update, we conduct extensive experiments and provide detailed results comparisons. The results from these experiments indicate the superiority of our ASH_+ .

Our main contributions are summarized below.

- We propose a novel adversarial approach, named Adversarial Semantic Hallucination+ (ASH_+), for single-source domain generalization. We leverage semantic information to adaptively hallucinate source domain images. Specifically, in ASH_+ , the spatial and class-wise information present in the semantic information is used to determine the absolute stylization strength, increasing the diversity of the generated training samples and improving the model generalization ability. Our approach is straightforward to implement and can be trained end-to-end.
- We conduct extensive experiments to demonstrate the effectiveness of our approach. We evaluate

1. The ASH_+ module is not necessary during inference, thereby avoiding additional computational costs.

our approach on the single-source domain generalization tasks with several benchmark datasets *i.e.* GTA5/Synthia→Cityscapes and the SYNTHIA dataset. ASH_+ demonstrates state-of-the-art performance for single-source domain generalization semantic segmentation. In particular, ASH_+ outperforms [18] by as much as 4.06% on the SYNTHIA dataset.

2 RELATED WORK

2.1 Domain Generalization

Prior works for domain generalization can be broadly classified into the following branches: data augmentation [15], [16], [19], [20], [21], representational learning [22], [23], and meta-learning [24], [25]. Data augmentation approaches typically vary the domain-variant features in the source domain data. Initial work such as Yue *et al.* [13] randomized the colour information of the source domain images via style transfer. However, preserving label and semantic information during data augmentation remains a key challenge. Excessive data augmentation may reduce correspondence between the ground truth labels and the data, causing the model to learn incorrect relationships between the data and the labels. Xu *et al.* [26] address this problem by limiting transformations to the low spatial frequency component of the source domain images. The domain-variant features, such as colour and texture information, generally reside in the low spatial frequency component of the images. Conversely, domain-invariant features such as shape information are located in the higher spatial frequency component of the images. Therefore, restricting transformations to the low spatial frequency component in the images ensures that original labels are preserved during transformation.

Representational learning approaches [22], [23] typically train the model to extract domain-invariant representations. Domain-invariant representations are generally assumed to be transferrable to other domains. Choi *et al.* [23] identify the domain-variant features (features that are covariance sensitive to image style transformation) and selectively whiten these features. However, it was shown that a model optimized to extract domain invariant representations, while simultaneously having a small error on the source domain data, is insufficient to guarantee good generalizability [27]. Zhao *et al.* [27] showed that minimizing loss on the target domain data is a sufficient condition for adaptation. Since target domain data are unavailable during training, this has led to work [24], [25] that attempts to estimate the distribution shift during training.

Meta-learning [24], [25] aims to achieve model generalizability by training the model to perform well on multiple tasks. This is done by separating the source domain training data into two parts: meta-train and meta-test data. The distribution shift between the meta-train and the meta-test approximates the domain shift between the source domain data and the unseen target domain data. Here, it is assumed that good performance on the meta-test data will translate to good model generalizability. Li *et al.* [24] split the source domain training data into meta-train and meta-test data as an approximation of the domain shift between the source domain data and the unseen target domain data. Qiao

et al. [25] extend this by using adversarially augmented source domain data as meta-test data, which would provide a better approximation of the unseen target domain data compared to the original source domain data.

2.2 Data Augmentation Via Style Transfer

Data augmentation is a widely used technique and it increases the size of training data through label-preserving transformations, such as randomized color jittering, image scaling, and shifting. As observed by Zeng *et al.* [28], data augmentation does not improve performance universally across different contexts and requires additional regularization to help ensure generality across different data. This perspective is further supported by Geirhos *et al.* [29] and they show that deep learning models that are pretrained on ImageNet data rely heavily on texture information, even when data augmentation is applied during training. To address this, Geirhos *et al.* [29] proposed that stylizing the ImageNet dataset significantly reduces the bias of pretrained models towards texture.

In the domain adaptation scenario, style transfer from target domain data to source domain data has been explored as a potential solution to overcome overfitting to domain-variant features [7], [30]. However, these methods require access to the target domain data and are not applicable in the domain generalization setting. To address this challenge, various methods [31], [32] that transfer styles from auxiliary datasets to the source domain training data have been proposed, resulting in improved model generalization. By transferring styles that are different from those of the source domain, these methods increase the diversity of the training data.

2.3 Style Transfer via Generative Models

Generative models, such as Generative Adversarial Networks (GANs) [33], are capable of synthesizing diverse data that closely match the distribution of the training data. Recently, several works [34], [35], [36] have shown that incorporating semantic information as a prior for a conditional GAN can significantly enhance the quality of synthesized images.

Wang *et al.* [35] demonstrated superior output image quality by introducing semantic information in the feature space during super-resolution. They regulate the transformation of the low-resolution image features with segmentation output from the low-resolution image as a prior, resulting in improved image quality. Similarly, Park *et al.* [34] also conditioned the generated image output with semantic information, which constrained the stylistic variations within the semantic boundaries. This approach not only increased the realism of the generated images but also allowed the user to control the layout within the generated images.

Finally, the recent work on image dehazing by Zhang *et al.* [36] further supports the effectiveness of using semantic information to condition image enhancement. They introduce a semantic-aware dehazing network that estimates the semantic prior. They then fuse the semantic prior with the extracted features from the hazy image to recover the obscured details in the hazy image. However, while the previous work [34], [35], [36] mentioned here use the

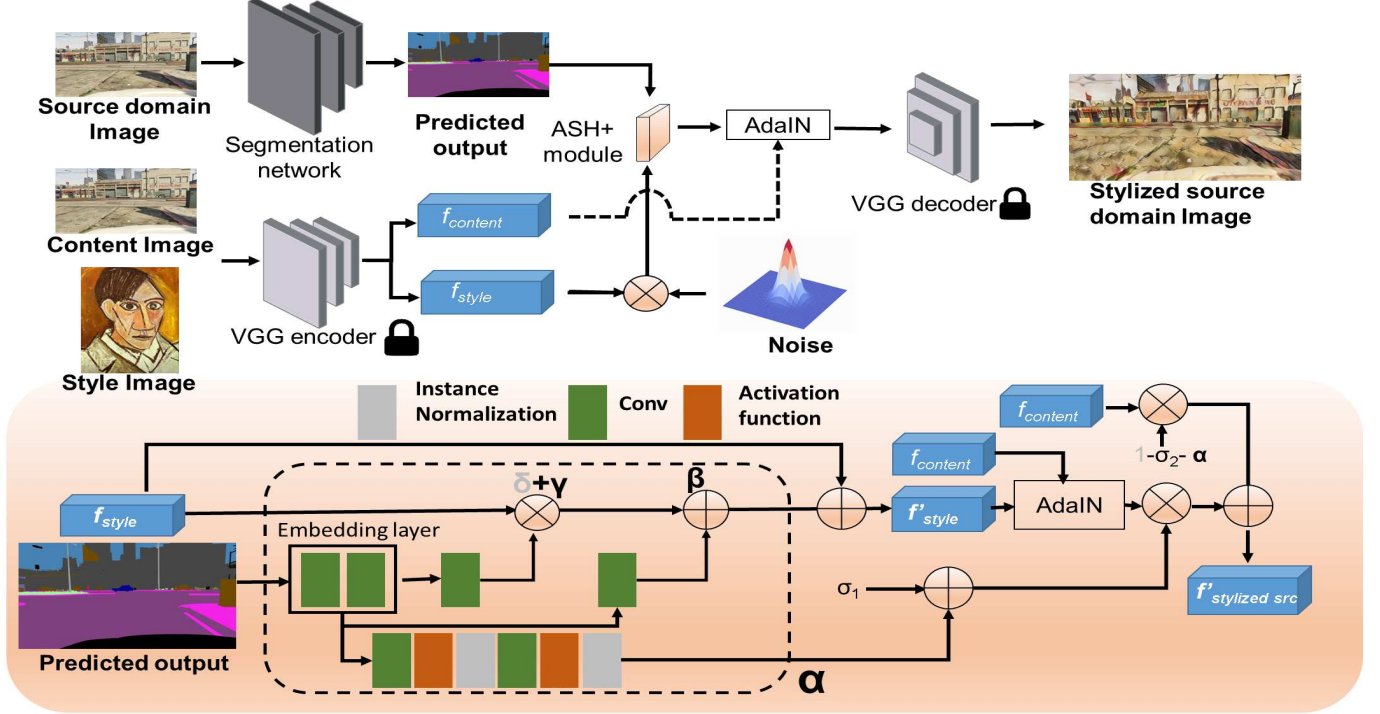


Fig. 2: Description of ASH_+ . We use the predicted output from the source domain image, together with the style features from a randomly selected image, as input to ASH_+ . The ASH_+ module then generates the element-wise scale γ , shift β and rebalancing α variables. γ and β both perturb the input style features to introduce additional variation, while α determines the element-wise proportion of the perturbed style features and content features in the reconstructed image. Different from earlier work [17] which uses a global hyperparameter, the element-wise rebalancing variable α allows for more fine-grained control over stylization. σ_1/σ_2 are both predefined hyperparameters.

semantic information to condition image generation and enhancement, we use the semantic information to generate challenging training data while preserving semantic details.

3 METHOD

In this section, we provide technical details on the Adversarial Semantic Hallucination+ (ASH_+) module designed to generate a diverse set of training data for domain-generalizable models. The structure of this section is as follows: Firstly, we provide a brief introduction to Adaptive Instance Normalization (AdaIN) [37]. Secondly, we elaborate on our module's architecture, objective functions, and learning details.

3.1 Preliminary background

Adaptive instance normalization [37] is a technique that preserves the content information of an image while incorporating the style from another image. This is achieved by first extracting the features from both the content and style images using a pre-trained VGG19 [38] encoder. The style features are then merged with the content features using the adaptive instance normalization operation, which normalizes the mean and variance of each feature map to match that of the style image while preserving the spatial information of the content image. Mathematically, the adap-

tive instance normalization operation can be expressed as follows:

$$\text{AdaIN}(f_{src}, f_{sty}) = \sigma(f_{sty}) \left(\frac{f_{src} - \mu(f_{src})}{\sigma(f_{src})} \right) + \mu(f_{sty}) \quad (1)$$

AdaIN re-normalizes the channel-wise mean $\mu(\cdot)$ and variance $\sigma(\cdot)$ of the content features (i.e. source features f_{src}) to match that of the style features f_{sty} .

3.2 Adversarial Semantic Hallucination+

Our framework consists of a segmentation module G , a semantic hallucination module ASH_+ , and a pre-trained VGG encoder/decoder, as shown in Figure 2. We denote the parameters for the segmentation network G and ASH_+ as θ_G and θ_{ASH} respectively.

Based on AdaIN, ASH_+ generates new training data via style transfer. Inspired by previous work [34], we condition the style transfer with semantic information. Specifically, we apply the semantic information present in the pixel-wise one-hot probability output P_{ij}^k of the source domain images X_s as a prior ϕ to condition the stylization:

$$\phi = (P_{ij}^1, P_{ij}^2, \dots, P_{ij}^k), \quad (2)$$

where k refers to the number of classes and ij refers to the spatial position in the image.

The pixel-level predictions $\phi \in \mathbb{R}^G$ are mapped to a latent space encoding $z_e \in \mathbb{R}^m$ via an embedding layer in

Algorithm 1 Adversarial approach for domain generalization

Input: Source domain data \mathbf{X}_s , Source domain label \mathbf{Y}_s , Style image \mathbf{X}_{style} , Segmentation network G , Pretrained Encoder Enc , Pretrained Decoder Dec , Adversarial Semantic Hallucination module ASH_+ , Adaptive Instance Normalization (AdaIN), Number of iterations $Iter_{num}$

Output: Optimized segmentation network for domain generalization

- 1: **for** $0, \dots, Iter_{num}$ **do**
- 2: Obtain \mathbf{f}_{src} via $Enc(\mathbf{X}_s)$.
- 3: Obtain \mathbf{f}_{style} via $Enc(\mathbf{X}_{style})$.
- 4: Obtain α , γ and β as shown in Eq. 3
- 5: Perturb \mathbf{f}_{style} with γ β as shown in Eq. 4
- 6: Merge source features \mathbf{f}_{src} and perturbed style features \mathbf{f}'_{style} with AdaIN.
- 7: Apply rebalancing coefficient α to balance the proportion of \mathbf{f}_{src} with the merged source-style features from step (6).
- 8: Generate stylized source image $\mathbf{X}_{stylized}$ by decoding the output from step (7) with Dec .
- 9: Train ASH_+ by minimizing $L_{ASH}(G, \mathbf{f}_{src}, \mathbf{f}'_{style})$.
- 10: Train G by minimizing $\mathcal{L}_{seg}(G, \mathbf{X}_s, \mathbf{Y}_s)$.
- 11: Train G by minimizing $\mathcal{L}_{cont}(\mathbf{X}_{stylized}, \mathbf{X}_s)$.
- 12: **end for**

ASH_+ . ASH_+ then generates the style-content rebalancing factor α , the classwise scaling γ , and the shifting β coefficients via the following equation:

$$\gamma, \beta, \alpha = ASH_+(\mathbf{z}_e), \quad (3)$$

where γ, β and α share the same spatial and channel dimensions as the style/content features ($N \times 512 \times H \times W$ in this work). The usage of style-content rebalancing factor α , the classwise scaling γ , and the shifting β coefficients will be explained as follows.

The style \mathbf{f}_{style} and content features \mathbf{f}_{src} are obtained from the style \mathbf{X}_{style} and the source \mathbf{X}_s images respectively via a pretrained VGG encoder. Previous work [39], [40] showed that adding noise to the inputs improves model generalizability. This is likely due to the regularizing effect of noise. Therefore, we applied noise \mathbf{z} orthogonal to the style features because we wanted to increase style feature diversity while preserving the original style information. Given the classwise scaling γ , and the shifting β , and noise \mathbf{z} , ASH_+ linearly transforms the style features \mathbf{f}_{style} via γ, β via the following equation:

$$\mathbf{f}'_{style} = \gamma(\mathbf{z} \cdot \mathbf{f}_{style} + 1) + \beta \quad (4)$$

By doing this, we control the stylization of image pixels depending on their spatial and class-wise properties. Perturbing the style features increases the diversity of the training data and can be considered to be a form of data augmentation.

To improve the adaptability of ASH_+ to each pixel's properties, we control stylization strength by determining the element-wise and channel-wise proportions of the original source features \mathbf{f}_{src} and the renormalized source features AdaIN($\mathbf{f}_{src}, \mathbf{f}_{sty}$) via the element-wise and channel-wise style-content rebalancing variable α . Specifically, we generate the stylized source domain images $\mathbf{X}_{stylized}$ with the following equation:

$$\mathbf{X}_{stylized} = Dec((\sigma'_1 + \alpha)\mathbf{f}_{src} + (\sigma'_2 - \alpha)\text{AdaIN}(\mathbf{f}_{src}, \mathbf{f}'_{style})), \quad (5)$$

where Dec is a pretrained decoder, AdaIN is the adaptive instance normalization equation defined in equation 1, σ'_1 and σ'_2 are two hyper-parameters.

3.3 Training Details

We train the two sub-modules in our framework, namely the segmentation network G and the ASH_+ module.

3.3.1 Optimization for the segmentation network G

The segmentation network G [9] is trained to minimize segmentation loss \mathcal{L}_{seg} and the pixel-wise consistency loss \mathcal{L}_{cont} . Segmentation loss $\mathcal{L}_{seg}(G, \mathbf{X}, \mathbf{Y})$ is derived from computing the cross entropy loss for the segmentation output [9]:

$$\mathcal{L}_{seg}(G, \mathbf{X}, \mathbf{Y}) = \sum_{i=1}^{H \times W} \sum_{c=1}^C -Y_{i,c} \log(G(X_{i,c})), \quad (6)$$

where $G(X_{i,c})$ refers to the predicted probability of class c on the i th pixel. $Y_{i,c}$ is the known ground truth probability for class c on the i th pixel, where $Y_{i,c} = 1$ if the pixel belongs to the class c and $Y_{i,c} = 0$ if otherwise.

The pixel-wise consistency loss function is based on the formulation from [41], which computes the Kullback-Leibler divergence between the pixel-wise segmentation output of the original source domain image and the segmentation output from the stylized source domain image. The pixel-wise consistency loss is given by the following equation:

$$\mathcal{L}_{cont}(G, \mathbf{X}_i^{stylized}, \mathbf{X}_i^s) = \frac{1}{H \times W} \sum_{i=1}^{H \times W} KL(G(\mathbf{X}_i^{stylized}) || G(\mathbf{X}_i^s)), \quad (7)$$

where $G(\mathbf{X}_i^{stylized})$ represents the class probabilities of the i th pixel in the segmentation output of the stylized source domain data, $G(\mathbf{X}_i^s)$ represents the class probabilities of the i th pixel in the segmentation output of the original source domain data, $KL(\cdot)$ is the Kullback-Leibler divergence between two probabilities, and $\mathbb{R} = 1, 2, \dots, H \times W$ denotes all the pixels in the segmentation output.

It is noted that this is different from the previous work [17], which uses a discriminator to distinguish between the segmentation output from the stylized source domain data and the segmentation output from the source domain data. We found that performance is comparable when we

replaced the discriminator with the pixelwise consistency loss instead. This modification further reduces the computational overhead required during training.

3.3.2 Optimization for ASH_+

We optimize the ASH_+ module by maximizing pixelwise consistency loss \mathcal{L}_{cont} . This encourages the ASH_+ module to create challenging training data for the segmentation network G . We minimize content loss \mathcal{L}_c from the source features to preserve the semantic information present in the source features. We also minimize style loss \mathcal{L}_s from the perturbed style features to maximize the stylistic diversity of the generated images. We compute the loss for ASH_+ with the following equation:

$$\begin{aligned} \mathcal{L}_{ASH_+}(G, f_{src}, f'_{style}, X_{stylized}, X_s) = & \\ & - \mathcal{L}_{cont}(G, X_{stylized}, X_s) \\ & + \mathcal{L}_c(f_{src}, \text{AdaIN}(f_{src}, f'_{style})) \\ & + \mathcal{L}_s(f'_{style}, \text{AdaIN}(f_{src}, f'_{style})) \\ & - \mathcal{L}_s(f_{src}, \text{AdaIN}(f_{src}, f'_{style})) \end{aligned} \quad (8)$$

We use the formula for content and style loss as defined in [37]. Content loss is derived from the L_2 norm between the original source domain features and the stylized features. Style loss is computed from the mean and standard deviation of the features extracted from each of the L convolution layers in the VGG encoder.

$$\mathcal{L}_c = \|f_{src} - \text{AdaIN}(f_{src}, f'_{style})\|_2 \quad (9)$$

$$\begin{aligned} \mathcal{L}_s = \sum_{i=1}^L & (\|\mu(f_{src}) - \mu(\text{AdaIN}(f_{src}, f'_{style}))\| \\ & + \|\sigma(f_{src}) - \sigma(\text{AdaIN}(f_{src}, f'_{style}))\|) \end{aligned} \quad (10)$$

Here, we minimize the amount of style information retained from the content images while simultaneously preserving semantic information from the original source domain images in the stylized images. The training workflow is summarized in Algorithm 1. It is noted that the weights for the pretrained encoder and decoder that are used during stylization are not updated during training. After finishing training, we only need the segmentation network G for evaluation and the ASH_+ module is not required after training.

4 EXPERIMENTS

To demonstrate the effectiveness of ASH_+ , we conducted extensive experiments on several widely used benchmarks.

4.1 Datasets

We evaluate our proposed method using the following publicly available datasets.

- **SYNTHIA** [43] is a synthetic semantic segmentation dataset of urban scenes with different weather and illumination levels, across 3 different environments (Highway, New York-like and Old European Town). We use the 13 semantic categories in the dataset. Similar to previous work [25], we use images from

Dawn/Spring/Fog in the Highway environment as the source domain. We train the models under each of the different weather conditions and evaluate them on the New York-like and Old European Town subsets.

- **GTA5** [47] is a synthetic semantic segmentation dataset with 24,966 densely annotated images with resolution 1914×1052 pixels, and has 19 categories that are compatible with the Cityscapes [48] dataset.
- **Synthia** [43] refers to the SYNTHIA-RAND-CITYSCAPES subset from the publicly available database for semantic segmentation. It has 9,400 densely annotated images with resolution 1280×760 pixels and has 16 categories that are compatible with the Cityscapes [48] dataset.
- **Cityscapes** [48] is a real world driving dataset with densely annotated images of resolution 2048×1024 pixels. We use the validation split of 500 densely annotated images to evaluate model performance.

We use 50,000 images from the ImageNet [49] validation data (ILSVRC2011) as a source of style images. We use the mean Intersection over Union (mIoU) to measure the segmentation performance, which is a widely used metric quantifying the overlap between the ground truth labels and the predicted output.

4.2 Implementation Details

For SYNTHIA, our implementation is based on the approach by Qiao *et al.* [25]. The training and testing images are from the left-front camera and are resized to 192×320 pixels. During training, we use the Adam [50] optimizer with a batch size of 8 images and a Fully Convolutional Network (FCN) [51], with a ImageNet pretrained ResNet-50 backbone. We first train the network on the source domain data for 50 epochs, followed by joint training with ASH_+ for a maximum of 10 epochs. We implement the model with the PyTorch library [52] on a single 12GB Titan X GPU.

For GTA5/Synthia→Cityscapes, we implement our approach with the PyTorch library [52] on a single 16GB Quadro RTX 5000. The GTA5 images are resized to 1280×720 pixels and the SYNTHIA images are resized to 1280×760 pixels. We use the Deeplab-v2 segmentation network [53] with ResNet-101 [54] backbone pretrained on the ImageNet dataset [55], following the implementation by Luo *et al.* [9]. We use stochastic gradient descent (SGD) with a momentum of 0.9 to optimize the segmentation network (Deeplab-v2) and ASH_+ module. The initial learning rate for the segmentation network is 2.5×10^{-4} . We train the network for 100,000 iterations.

4.3 Comparison with Competing methods

SYNTHIA Here, we seek to evaluate the generalizability of ASH_+ across different weather conditions and environments. While the domain gap between the synthetic and real-world images may be larger compared to this experimental setting, this task evaluates the generalization performance on multiple unseen target domain domains (>2), compared to the previous setting (GTA5/Synthia→Cityscapes) which evaluates performance on a

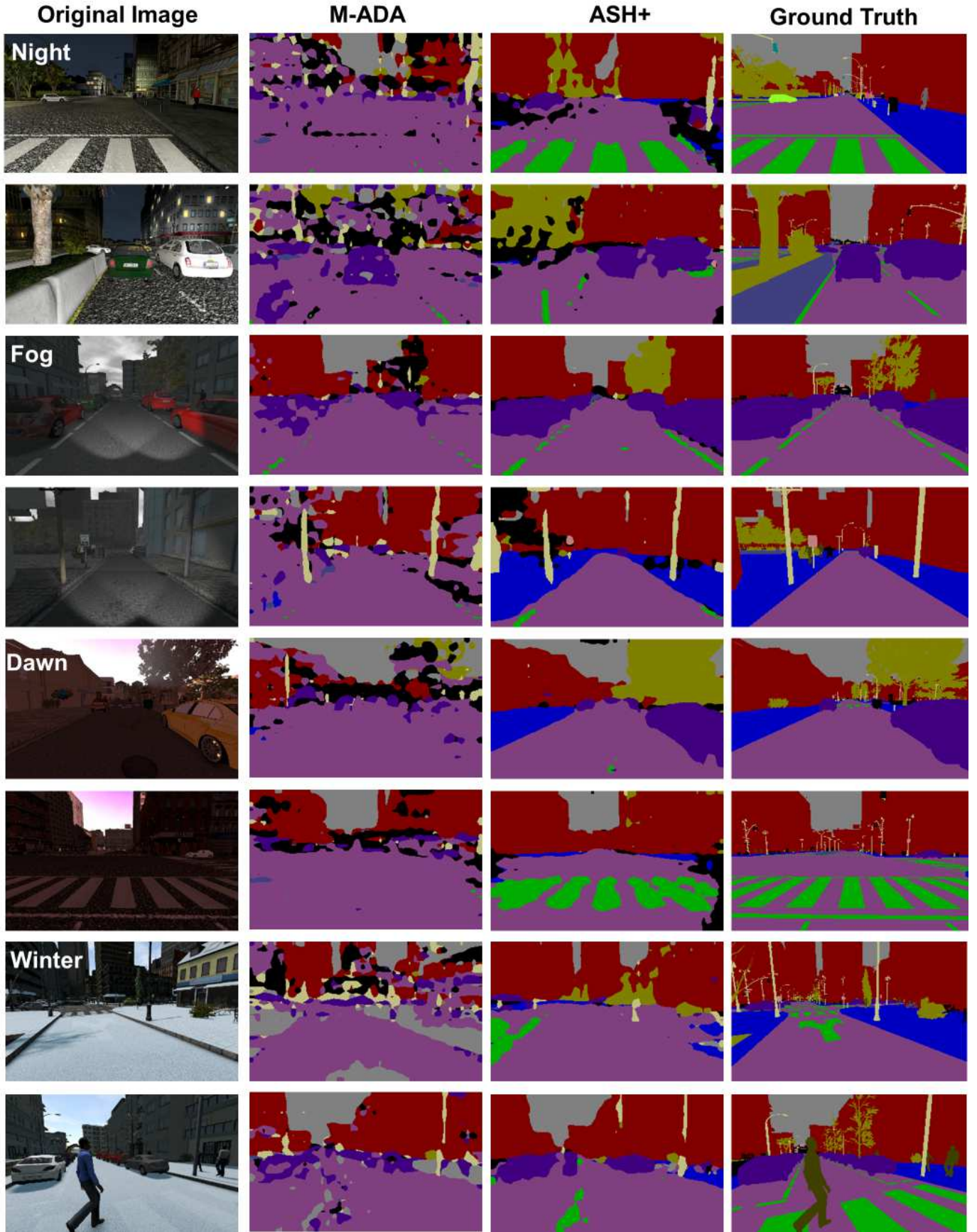


Fig. 3: Qualitative comparison of segmentation output for SYNTHIA. For each image, we show the corresponding results for “M-ADA” [25], our proposed method ASH_+ on the original image and the corresponding ground truth. The model used was trained on Highway (Spring) and the results on the unseen weather conditions (Night, Fog, Dawn and Winter) are shown.

New York												Old European Town						
Source Domain	Method	Dawn	Fog	Night	Spring	Winter	Dawn	Fog	Night	Spring	Winter	Avg						
Highway (Dawn)	ERM [42]	27.80	2.73	0.93	6.80	1.65	52.78	31.37	15.86	33.78	13.35	18.70						
	M-ADA [25]	29.10	4.43	4.75	14.13	4.97	54.28	36.04	23.19	37.53	14.87	22.33						
	PDEN [18]	30.63	21.74	16.76	26.10	19.91	54.93	47.55	36.97	43.98	23.83	32.24						
	Source-only	24.50	2.90	0.40	1.80	0.06	53.90	33.50	18.00	30.9	12.80	17.90						
	<i>ASH</i> ₊	30.70	30.00	27.30	31.20	27.30	52.30	50.10	43.50	45.60	25.00	36.30						
Highway (Fog)	ERM [42]	17.24	34.80	12.36	26.38	11.81	33.73	55.03	26.19	41.74	12.32	27.16						
	M-ADA [25]	21.74	32.00	9.74	26.40	13.28	42.79	56.60	31.79	42.77	12.85	29.00						
	PDEN [18]	25.61	35.16	17.05	32.45	21.03	45.67	54.91	37.38	48.29	20.80	33.83						
	Source-only	18.80	34.70	12.50	26.30	13.20	36.10	54.00	28.80	42.00	14.10	28.05						
	<i>ASH</i> ₊	25.60	36.20	19.40	31.80	27.30	42.30	54.70	37.00	44.00	27.10	34.54						
Highway (Spring)	ERM [42]	26.75	26.41	18.22	32.89	24.60	51.72	51.85	35.65	54.00	28.13	35.02						
	M-ADA [25]	29.70	31.03	22.22	38.19	28.29	53.57	51.83	38.98	55.63	25.29	37.47						
	PDEN [18]	28.17	27.67	27.53	34.30	28.85	53.75	51.53	46.87	55.63	30.61	38.49						
	Source-only	27.10	27.70	15.90	31.60	25.00	52.50	50.50	33.50	54.90	28.30	34.70						
	<i>ASH</i> ₊	34.40	36.50	32.60	40.60	29.00	52.60	54.80	49.40	55.80	28.20	41.39						

TABLE 1: Quantitative semantic segmentation results on SYNTHIA [43]. The models are trained using a single-source domain and evaluated on several unseen target domains. We report the mean Intersection Over Union (mIoU) and also show the visual results in Figure 7

GTA5 → Cityscapes																						
	Year	Arch.	road	side.	buil.	wall	fence	pole	light	sign	vege.	terr.	sky	pers.	rider	car	truck	bus	train	motor	bike	mIoU
Source only	-	R	75.8	16.8	77.2	12.5	21.0	25.5	30.1	20.1	81.3	24.6	70.3	53.8	26.4	49.9	17.2	25.9	6.5	25.3	36.0	36.6
Fully supervised	-	R	97.9	81.3	90.3	48.8	47.4	49.6	57.9	67.3	91.9	69.4	94.2	79.8	59.8	93.7	56.5	67.5	57.5	68.8	70.4	
Domain Generalization																						
Advent [44]	2019	R	83.00	1.80	72.00	8.20	3.60	16.20	22.90	9.80	79.30	17.10	75.70	35.10	15.80	70.90	30.90	35.30	0.00	16.40	24.90	32.60
MaxSquare [45]	2019	R	76.80	14.20	77.00	18.80	14.10	14.50	30.30	18.00	79.30	11.70	70.50	53.00	24.20	68.70	25.30	14.00	1.30	20.60	25.50	34.60
CLAN [9]	2019	R	87.20	20.10	77.90	25.60	19.70	23.00	30.40	22.50	76.80	25.20	76.20	55.10	28.10	82.70	30.70	36.90	0.80	26.00	17.10	40.10
ASM [7]	2020	R	56.20	0.00	7.00	0.60	1.00	0.30	0.70	0.60	13.80	0.10	0.01	0.08	0.04	1.20	0.50	0.70	0.20	0.00	0.00	4.40
Domain Rand. [13]	2019	R	-	-	-	-	-	-	-	-	-	-	-	-	-	-	-	-	-	-	42.53	
<i>ASH</i> ₊	2022	R	85.24	21.37	78.59	25.37	12.14	24.10	31.30	27.84	81.30	29.45	77.01	56.89	25.52	79.00	33.68	32.96	3.22	20.66	23.06	40.46
SOMAN [46]	2021	R	-	-	-	-	-	-	-	-	-	-	-	-	-	-	-	-	-	-	45.90	

TABLE 2: Segmentation performance of Deeplab-v2 with ResNet-101 backbone trained on GTA5, tested on Cityscapes.

single unseen target domain. We compare our method with a few state-of-the art works, namely M-ADA [25] and PDEN [18]. Both methods increase the diversity of the training data by transforming the data. Qiao *et al.* [25] apply a Wasserstein Autoencoder together with a relaxation loss function, which maximizes the difference between the transformed data and original source data. The task model is then updated to minimize loss on the original source data (meta-train) and the transformed data (meta-test). The Wasserstein Autoencoder requires additional computational memory overhead, with 10^9 parameters while our module uses 100x fewer parameters to generate stylized images. Li *et al.* [18] progressively generate data that estimates the style and colour information present in the unseen target domain data, followed by contrastive learning to help the model learn good domain-invariant representations for the different classes. The quantitative results are shown in Table 1 and a qualitative comparison is shown in Figure 3. For all three settings (Highway-Dawn/Fog/Spring), *ASH*₊ yields state-of-the-art performance compared to recent work [18], [25], further validating the effectiveness of *ASH*₊ for domain generalization tasks.

Cityscapes We compare our method with DRPC [13] and SOMA [46]. Both methods generate additional data from the source domain images to improve model generalizability. DRPC [13] generates multiple stylized images from a single-source domain image per iteration and trains the model to maximize consistency between the extracted features from the differently stylized images via a spatial pyramidal pooling approach. The rationale behind their approach is that model output should be consistent regardless of any variations in image style, colour information or texture within the input images. They also randomize the scale of the input images during training to maximize model generalizability to different object scales and object layouts within the input, since these aspects may vary widely across domains. However, their method requires a large batch size of stylized training images (n=15). In contrast, our method only uses a batch size of 1, which reduces computational costs. Furthermore, the pyramidal pooling approach [13] is a feature-based loss and requires additional computational costs for comparison of the extracted features across each batch. In contrast, our approach computes the pixelwise consistency between the predicted output for the original

Synthia → Cityscapes																	
	Year	Arch.	road	side.	buil.	light	sign	vege.	sky	pers.	rider	car	bus	motor	bike	mIoU	mIoU16
Source only	-	R	47.10	19.50	68.90	9.10	9.30	75.10	79.10	52.50	20.30	43.00	20.70	9.40	29.30	37.17	32.38
Fully supervised	-	R	95.10	72.90	87.30	46.70	57.20	87.10	92.10	74.20	35.00	92.10	49.30	53.20	68.80	70.10	-
Domain Generalization																	
Advent [44]	2019	R	72.30	30.70	65.20	4.10	5.40	58.20	77.20	50.40	10.10	70.00	13.20	4.00	27.90	37.60	31.80
MaxSquare [45]	2019	R	57.80	23.19	73.63	8.37	11.66	73.84	81.92	56.68	20.73	52.18	14.71	8.37	39.18	40.17	34.96
CLAN [9]	2019	R	63.90	25.90	72.10	14.30	12.00	72.50	78.70	52.70	14.50	62.20	25.10	10.40	26.50	40.90	34.90
ASM [7]	2020	R	75.40	18.50	66.60	0.10	0.80	67.00	77.80	15.60	0.50	11.40	1.30	0.03	0.20	25.80	21.60
Domain Rand. [13]	2019	R	-	-	-	-	-	-	-	-	-	-	-	-	-	-	37.58
SoMAN [46]	2021	R	-	-	-	-	-	-	-	-	-	-	-	-	-	46.7	40.10
ASH ₊	2022	R	76.29	30.64	75.54	17.44	17.55	73.25	77.17	53.43	22.18	75.75	31.80	11.89	37.31	46.17	39.80

TABLE 3: Segmentation performance of Deeplab-v2 with ResNet-101 backbone trained on Synthia, tested on Cityscapes.

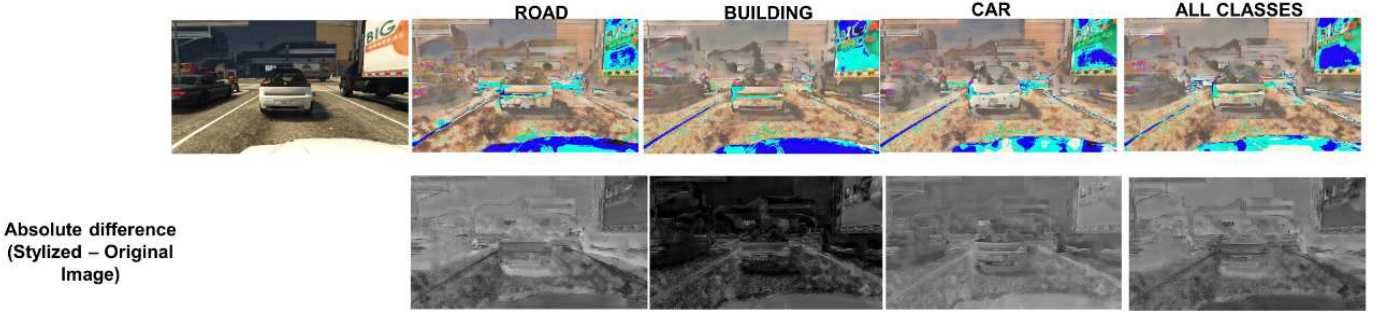


Fig. 4: Visualization of absolute stylization differences across classes for a single test image. For the classes listed (*i.e.* road, building and car), we exclude all other 18 classes in the segmentation output and stylize the source domain image only with the prediction outputs for that specified class. The absolute difference between the stylized image and the original source domain image is shown in the bottom row. The stylized image with semantic information from all classes is indicated as “all classes” in the rightmost column.

source domain image and the predicted output for the stylized source domain image. Since the image output is of lower dimensionality compared the extracted features, this further reduces the computational costs associated with our method. SOMAN [46] is a source-free domain adaptation approach, which pretrains a model on labeled source domain data in the first phase and applies several image transformations to maximize model generalizability. The second phase involves training the pretrained model on unlabeled target domain data, without any access to the source domain data. This differs from UDA (unsupervised domain adaptation), which trains the model with the labeled source domain data and the target domain data simultaneously. Therefore, it is critical for the pretrained model to generalize well to the target domain data because source free domain adaptation approaches rely on self supervised methods, where pseudo labels (labels generated from model predictions on the unlabeled target domain data) are used for training. We present the results on GTA5 →Cityscapes in **Table 2** and Synthia →Cityscapes in **Table 3**. The results indicate that *ASH₊* is competitive with state of the art work.

4.4 Feature Distribution Visualizations

We visualize the distributions of the feature representations in latent space. We randomly sampled 10,000 pixels from 40

randomly selected images from the target domain data (*i.e.* Cityscapes) and obtain the extracted feature representations from a baseline model trained only on source domain data (NoAdapt) and a model trained using our method. As seen in **Figure 5**, the feature representations from the different classes for our approach show better separation compared to the feature representations from ‘NoAdapt’.

4.5 Parameter Studies

We aim to determine: 1) the impact of data augmentation strength (proportion of original source domain content features to style features in the stylized image) on model performance and generalizability 2) how the style-content balancing factor α helps to modulate the stylization. We study the effects of varying the hyperparameters σ_1/σ_2 . Firstly, we vary the values for σ_1/σ_2 . While α is mostly sparse, with the mean close to 0, we observed that some values are approximately 1. This would mean that there would be limited information from the source domain images in those regions where α is close to zero. Therefore, setting σ_1/σ_2 is essential to ensuring that the source domain information is preserved during stylization. We conducted a series of experiments to determine the optimal σ_1/σ_2 values for SYNTHIA as shown in table 4 and GTA5 →Cityscapes as shown in table 5. For the SYNTHIA dataset, we found that the performance is better when a larger proportion

of the reconstructed image corresponds to the style features f_{sty} . However, for GTA5→Cityscapes, better task performance was observed when the initial proportions of the style and content features are approximately balanced. This may be caused by the greater variation in appearance among the SYNTHIA data(e.g. Spring →Winter) compared to GTA→Cityscapes.

Class-wise differences To further establish the case for class-wise differences in data augmentation, we conducted an experiment where we limited the semantic information from the segmentation output to a single class. This means that the ASH_+ module would only be provided with the predicted probabilities corresponding to a particular class. We then obtained the absolute difference in image intensities between the stylized image and the original source domain image. Since the number of pixels predicted may vary widely across classes, we normalized the absolute image intensity difference by the number of predicted pixels corresponding to that class. As shown in **Figure 4**, the relative change in intensities varies across classes, with larger variations in image intensities for classes such as 'road' compared to classes such as 'building'. We suggest that 'road' pixels are generally easier to classify compared to 'building' pixels, leading to a larger change in pixel intensity. Additionally, α is inversely proportional to the stylization strength in the stylized source domain images since it determines the spatial and channel-wise proportion of the original source domain features to the perturbed style features. Regions that have high prediction entropy, such as object boundaries, generally have larger $|\alpha|$ compared to regions with lower prediction entropy. This leads us to suggest that α imposes an upper bound on stylization for regions that are difficult to classify. We also observe that

σ_1	0	0.25	0.5	0.75
σ_2	1	0.75	0.5	0.25
Avg. mIoU	41.39	40.54	28.37	20.92

TABLE 4: Hyperparameter evaluation with the SYNTHIA Dataset. The model was trained on Highway-Spring and the performance on the other 10 datasets from New York-like and Old European Town are averaged.

$|\alpha|$ decreases for classes such as 'road' and building while remaining relatively consistent for other classes such as 'person'. This is likely due to the progressively increasing augmentation for these classes, suggesting that ASH_+ determines stylization strength based on the class information.

4.6 Ablation Study

We evaluate the contribution of the different components by conducting an ablation study for Synthia→Cityscapes (Table 6). The results indicate that while stylization improves performance relative to the baseline, it is still markedly

σ_1	0.1	0.4	0.5	0.6	0.7	0.75	0.25
σ_2	0.9	0.6	0.5	0.4	0.3	1.5	0.5
mIoU	38.62	39.04	40.46	40.22	39.41	35.70	39.61

TABLE 5: Hyperparameter evaluation for GTA5→Cityscapes.

Baseline	Stylization	Orthogonal Noise	ASH_+	α	mIoU
✓					32.38
✓	✓				36.24
✓	✓	✓			37.98
✓	✓	✓	✓		38.88
✓	✓	✓	✓	✓	39.80

TABLE 6: Ablation study for Synthia→Cityscapes. The baseline approach is the CLAN [9] method trained on source domain data. Stylization refers to the model trained with additional stylized data, ASH_+ [17] is our previous work and α refers to the spatial-wise rebalancing factor.

lower relative to the state-of-the-art performance. This suggests that the stylization process can be optimized further. We then introduced orthogonal noise to the style features. This preserves the original style information while simultaneously perturbing the style features to increase diversity. The results suggest introducing orthogonal noise accounts for a modest improvement. Notably, the results improved considerably after introducing ASH_+ with the style-content rebalancing variable α . Since ASH_+ previously used an empirically determined global hyperparameter to control the extent of stylization, this highlights the importance of modulating the stylization strength.

5 CONCLUSION

In this paper, we introduce ASH_+ (adversarial style hallucination) with the goal of addressing the problem of modulating data augmentation strength in domain generalization. By leveraging the semantic information, ASH_+ perturbs the input style features before fusing the perturbed style features with the source domain features. Additionally, we introduce a novel learned parameter which balances the proportion of content features and the perturbed style features. This parameter is also derived from the semantic information present in the segmentation output. Experimental results demonstrate the effectiveness of ASH_+ , which yields competitive segmentation performance compared with state-of-the-art domain generalization approaches.

ACKNOWLEDGMENTS

GRANT This work was supported by the A*STAR Computational Resource Centre through the use of its high performance computing facilities and was also partially performed on resources of the National Supercomputing Centre, Singapore (<https://www.nscc.sg>).

REFERENCES

- [1] A. Krizhevsky, I. Sutskever, and G. E. Hinton, "Imagenet classification with deep convolutional neural networks," *Commun. ACM*, vol. 60, no. 6, p. 84–90, may 2017. [Online]. Available: <https://doi.org/10.1145/3065386>
- [2] G. Hinton, L. Deng, D. Yu, G. E. Dahl, A.-r. Mohamed, N. Jaitly, A. Senior, V. Vanhoucke, P. Nguyen, T. N. Sainath, and B. Kingsbury, "Deep neural networks for acoustic modeling in speech recognition: The shared views of four research groups," *IEEE Signal Processing Magazine*, vol. 29, no. 6, pp. 82–97, 2012.

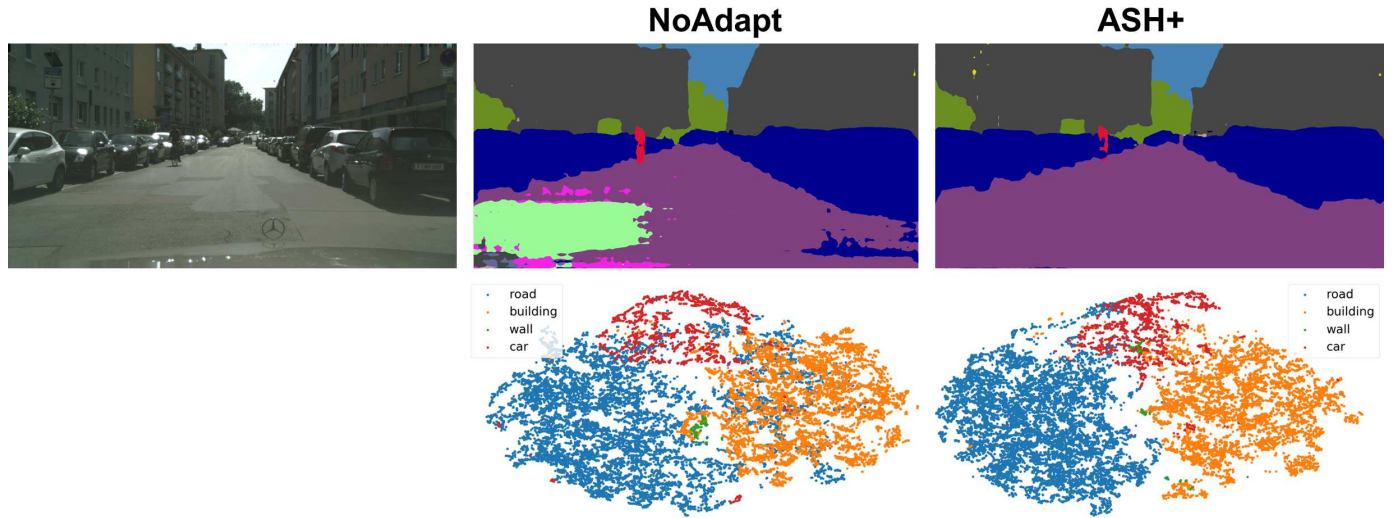


Fig. 5: t-SNE plots for NoAdapt (model trained on source domain data without any data augmentation or domain generalization approaches) and our approach. A representative segmentation output from each model is included.

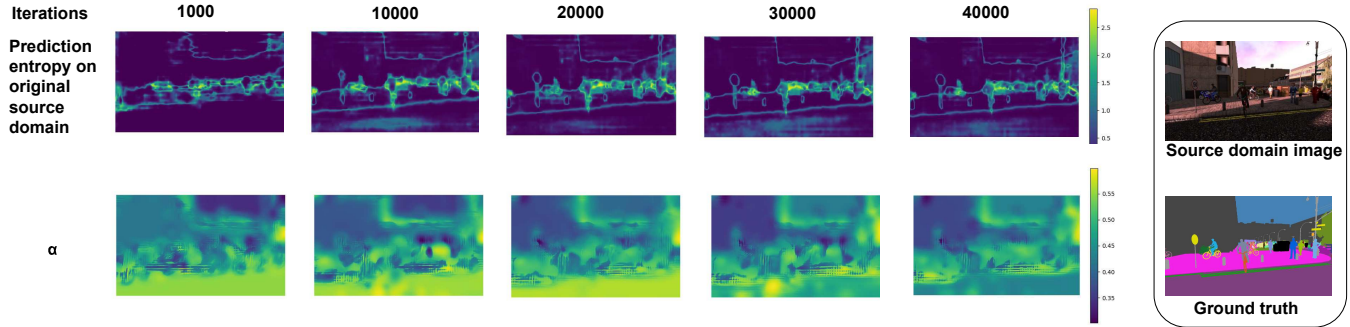


Fig. 6: Variations in $|\alpha|$ during training. α varies depending on class and spatial location. For example, α for the 'road' classes are generally higher relative to α for other classes such as 'building'.

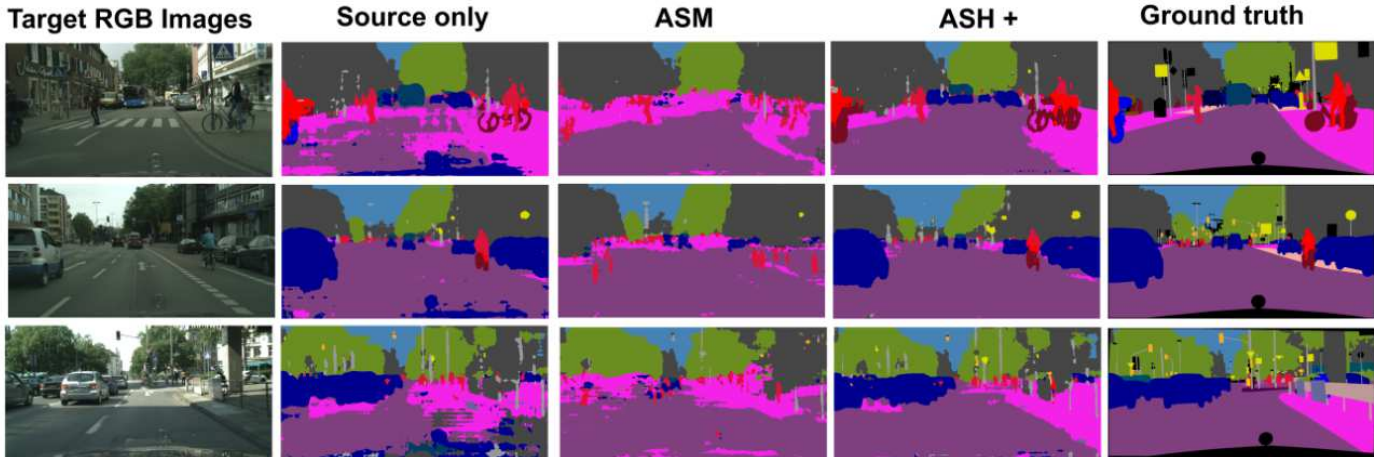


Fig. 7: Qualitative comparison of segmentation output for SYNTHIA \rightarrow Cityscapes. For each target domain image, we show the corresponding results for "Source only", "ASM" Adversarial Style Mining [7], "ASH+"(our proposed method) and the ground truth labels.

[3] I. Sutskever, O. Vinyals, and Q. V. Le, "Sequence to sequence learning with neural networks," in *Advances in Neural Information Processing Systems*, Z. Ghahramani, M. Welling, C. Cortes, N. Lawrence, and K. Weinberger, Eds., vol. 27. Curran Associates, Inc., 2014. [Online]. Available: <https://proceedings.neurips.cc/paper/2014/file/a14ac55a4f27472c5d894e2018c743d2-Paper.pdf>

[4] A. Yakimovich, A. Beaugnon, Y. Huang, and E. Ozkirimli, "Labels in a haystack: Approaches beyond supervised learning in biomedical applications," *Patterns*, 2021.

[5] X. Wang, H. Chen, C. Gan, H. Lin, Q. Dou, E. Tsougenis, Q. Huang, M. Cai, and P.-A. Heng, "Weakly supervised deep learning for whole slide lung cancer image analysis," *IEEE Transactions on Cybernetics*, vol. 50, no. 9, pp. 3950–3962, 2020.

[6] K. Zhou, Z. Liu, Y. Qiao, T. Xiang, and C. C. Loy, "Domain generalization: A survey," *IEEE Transactions on Pattern Analysis and Machine Intelligence*, pp. 1–20, 2022.

[7] Y. Luo, P. Liu, T. Guan, J. Yu, and Y. Yang, "Adversarial style mining for one-shot unsupervised domain adaptation," in *Advances in Neural Information Processing Systems*, 2020.

[8] Y. Ganin, E. Ustinova, H. Ajakan, P. Germain, H. Larochelle, F. Laviolette, M. Marchand, and V. S. Lempitsky, "Domain-adversarial training of neural networks," in *Domain Adaptation in Computer Vision Applications*, ser. Advances in Computer Vision and Pattern Recognition, 2017.

[9] Y. Luo, L. Zheng, T. Guan, J. Yu, and Y. Yang, "Taking a closer look at domain shift: Category-level adversaries for semantics consistent domain adaptation," in *Proceedings of the IEEE/CVF Conference on Computer Vision and Pattern Recognition (CVPR)*, 2019.

[10] M. Long, Z. CAO, J. Wang, and M. I. Jordan, "Conditional adversarial domain adaptation," in *Advances in Neural Information Processing Systems*, S. Bengio, H. Wallach, H. Larochelle, K. Grauman, N. Cesa-Bianchi, and R. Garnett, Eds., vol. 31, 2018.

[11] J. Dong, Y. Cong, G. Sun, Z. Fang, and Z. Ding, "Where and how to transfer: Knowledge aggregation-induced transferability perception for unsupervised domain adaptation," *IEEE Transactions on Pattern Analysis and Machine Intelligence*, pp. 1–1, 2021.

[12] Z. Gao, Y. Zhao, H. Zhang, D. Chen, A.-A. Liu, and S. Chen, "A novel multiple-view adversarial learning network for unsupervised domain adaptation action recognition," *IEEE Transactions on Cybernetics*, vol. 52, no. 12, pp. 13 197–13 211, 2022.

[13] X. Yue, Y. Zhang, S. Zhao, A. Sangiovanni-Vincentelli, K. Keutzer, and B. Gong, "Domain randomization and pyramid consistency: Simulation-to-real generalization without accessing target domain data," in *Proceedings of the IEEE/CVF International Conference on Computer Vision (ICCV)*, 2019.

[14] K. Li, Y. Zhang, K. Li, and Y. Fu, "Adversarial feature hallucination networks for few-shot learning," in *Proceedings of the IEEE/CVF Conference on Computer Vision and Pattern Recognition (CVPR)*, June 2020.

[15] M. Uzair and A. Mian, "Blind domain adaptation with augmented extreme learning machine features," *IEEE Transactions on Cybernetics*, vol. 47, no. 3, pp. 651–660, 2017.

[16] K. Zhou, Y. Yang, Y. Qiao, and T. Xiang, "Domain generalization with mixstyle," in *ICLR*, 2021.

[17] G. Tjio, P. Liu, J. T. Zhou, and R. S. M. Goh, "Adversarial semantic hallucination for domain generalized semantic segmentation," in *Proceedings of the IEEE/CVF Winter Conference on Applications of Computer Vision (WACV)*, 2022.

[18] L. Li, K. Gao, J. Cao, Z. Huang, Y. Weng, X. Mi, Z. Yu, X. Li, and B. Xia, "Progressive domain expansion network for single domain generalization," in *Proceedings of the IEEE/CVF Conference on Computer Vision and Pattern Recognition (CVPR)*, 2021.

[19] L. Zhang, X. Wang, D. Yang, T. Sanford, S. Harmon, B. Turkbey, B. J. Wood, H. Roth, A. Myronenko, D. Xu, and Z. Xu, "Generalizing deep learning for medical image segmentation to unseen domains via deep stacked transformation," *IEEE Transactions on Medical Imaging*, vol. 39, no. 7, pp. 2531–2540, 2020.

[20] R. Volpi, H. Namkoong, O. Sener, J. C. Duchi, V. Murino, and S. Savarese, "Generalizing to unseen domains via adversarial data augmentation," in *Advances in Neural Information Processing Systems*, S. Bengio, H. Wallach, H. Larochelle, K. Grauman, N. Cesa-Bianchi, and R. Garnett, Eds., vol. 31. Curran Associates, Inc., 2018. [Online]. Available: https://proceedings.neurips.cc/paper_files/paper/2018/file/1d941030763b3111f8802b48f151b14.pdf

[21] S. Shankar, V. Piratla, S. Chakrabarti, S. Chaudhuri, P. Jyothi, and S. Sarawagi, "Generalizing across domains via cross-gradient training," in *International Conference on Learning Representations*, 2018. [Online]. Available: <https://openreview.net/forum?id=r1Dx7fbCW>

[22] H. Li, S. J. Pan, S. Wang, and A. C. Kot, "Domain generalization with adversarial feature learning," in *Proceedings of the IEEE Conference on Computer Vision and Pattern Recognition (CVPR)*, June 2018. [Online]. Available: <https://openreview.net/forum?id=2018c743d2-Paper.pdf>

[23] S. Choi, S. Jung, H. Yun, J. T. Kim, S. Kim, and J. Choo, "Robustnet: Improving domain generalization in urban-scene segmentation via instance selective whitening," in *Proceedings of the IEEE/CVF Conference on Computer Vision and Pattern Recognition (CVPR)*, 2021.

[24] D. Li, Y. Yang, Y.-Z. Song, and T. Hospedales, "Learning to generalize: Meta-learning for domain generalization," *Proceedings of the AAAI Conference on Artificial Intelligence*, vol. 32, no. 1, Apr. 2018. [Online]. Available: <https://ojs.aaai.org/index.php/AAAI/article/view/11596>

[25] F. Qiao, L. Zhao, and X. Peng, "Learning to learn single domain generalization," in *Proceedings of the IEEE Conference on Computer Vision and Pattern Recognition (CVPR)*, 2020.

[26] Q. Xu, R. Zhang, Y. Zhang, Y. Wang, and Q. Tian, "A fourier-based framework for domain generalization," in *Proceedings of the IEEE/CVF Conference on Computer Vision and Pattern Recognition (CVPR)*, 2021.

[27] H. Zhao, R. T. D. Combes, K. Zhang, and G. Gordon, "On learning invariant representations for domain adaptation," in *Proceedings of the 36th International Conference on Machine Learning*, ser. Proceedings of Machine Learning Research, K. Chaudhuri and R. Salakhutdinov, Eds., vol. 97. PMLR, 09–15 Jun 2019, pp. 7523–7532. [Online]. Available: <https://proceedings.mlr.press/v97/zhao19a.html>

[28] S. Zeng, B. Zhang, J. Gou, and Y. Xu, "Regularization on augmented data to diversify sparse representation for robust image classification," *IEEE Transactions on Cybernetics*, vol. 52, no. 6, pp. 4935–4948, 2022.

[29] R. Geirhos, P. Rubisch, C. Michaelis, M. Bethge, F. A. Wichmann, and W. Brendel, "Imagenet-trained cnns are biased towards texture; increasing shape bias improves accuracy and robustness," in *International Conference on Learning Representations*, 2018.

[30] J. Hoffman, E. Tzeng, T. Park, J.-Y. Zhu, P. Isola, K. Saenko, A. Efros, and T. Darrell, "CyCADA: Cycle-consistent adversarial domain adaptation," in *Proceedings of the 35th International Conference on Machine Learning*. [Online]. Available: <http://proceedings.mlr.press/v80/hoffman18a.html>

[31] S. Zakharov, W. Kehl, and S. Ilic, "Deceptionnet: Network-driven domain randomization," in *Proceedings of the IEEE/CVF International Conference on Computer Vision (ICCV)*, October 2019.

[32] J. Tobin, R. Fong, A. Ray, J. Schneider, W. Zaremba, and W. Abbeel, "Domain randomization for transferring deep neural networks from simulation to the real world," in *IEEE/RSJ International Conference on Intelligent Robots and Systems (IROS)*, 2017.

[33] I. Goodfellow, J. Pouget-Abadie, M. Mirza, B. Xu, D. Warde-Farley, S. Ozair, A. Courville, and Y. Bengio, "Generative adversarial nets," in *Advances in Neural Information Processing Systems*, vol. 27, 2014.

[34] T. Park, M.-Y. Liu, T.-C. Wang, and J.-Y. Zhu, "Semantic image synthesis with spatially-adaptive normalization," in *Proceedings of the IEEE/CVF Conference on Computer Vision and Pattern Recognition (CVPR)*, 2019.

[35] X. Wang, K. Yu, C. Dong, and C. C. Loy, "Recovering realistic texture in image super-resolution by deep spatial feature transform," in *Proceedings of the IEEE/CVF Conference on Computer Vision and Pattern Recognition (CVPR)*, 2018.

[36] S. Zhang, W. Ren, X. Tan, Z.-J. Wang, Y. Liu, J. Zhang, X. Zhang, and X. Cao, "Semantic-aware dehazing network with adaptive feature fusion," *IEEE Transactions on Cybernetics*, vol. 53, no. 1, pp. 454–467, 2023.

[37] X. Huang and S. Belongie, "Arbitrary style transfer in real-time with adaptive instance normalization," in *Proceedings of the IEEE/CVF International Conference on Computer Vision (ICCV)*, 2017.

[38] K. Simonyan and A. Zisserman, "Very deep convolutional networks for large-scale image recognition," in *International Conference on Learning Representations*, 2015.

[39] G. An, "The effects of adding noise during backpropagation training on a generalization performance," *Neural Computation*, 1996.

[40] 763b3111f8802b48f151b14.pdf is equivalent to tikhonov regularization," *Neural Computation*, 1995.

[41] Y. Liu, K. Chen, C. Liu, Z. Qin, Z. Luo, and J. Wang, "Structured knowledge distillation for semantic segmentation," in *2019*

IEEE/CVF Conference on Computer Vision and Pattern Recognition (CVPR), 2019, pp. 2599–2608.

[42] V. Koltchinskii, *Oracle inequalities in empirical risk minimization and sparse recovery problems: École D'Été de Probabilités de Saint-Flour XXXVIII-2008*. Springer Science & Business Media, 2011, vol. 2033.

[43] G. Ros, L. Sellart, J. Materzynska, D. Vazquez, and A. Lopez, "The SYNTHIA Dataset: A large collection of synthetic images for semantic segmentation of urban scenes," in *Proceedings of the IEEE/CVF Conference on Computer Vision and Pattern Recognition (CVPR), 2016*.

[44] T.-H. Vu, H. Jain, M. Bucher, M. Cord, and P. Perez, "Advent: Adversarial entropy minimization for domain adaptation in semantic segmentation," in *Proceedings of the IEEE/CVF Conference on Computer Vision and Pattern Recognition (CVPR), 2019*.

[45] M. Chen, H. Xue, and D. Cai, "Domain adaptation for semantic segmentation with maximum squares loss," in *Proceedings of the IEEE/CVF International Conference on Computer Vision (ICCV), 2019*.

[46] J. N. Kundu, A. Kulkarni, A. Singh, V. Jampani, and R. V. Babu, "Generalize them adapt: Source-free domain adaptive semantic segmentation," in *Proceedings of the IEEE/CVF International Conference on Computer Vision (ICCV), 2021*, pp. 7046–7056.

[47] S. R. Richter, V. Vineet, S. Roth, and V. Koltun, "Playing for data: Ground truth from computer games," in *Proceedings of the European Conference on Computer Vision (ECCV), 2016*.

[48] M. Cordts, M. Omran, S. Ramos, T. Rehfeld, M. Enzweiler, R. Benenson, U. Franke, S. Roth, and B. Schiele, "The cityscapes dataset for semantic urban scene understanding," in *Proceedings of the IEEE/CVF Conference on Computer Vision and Pattern Recognition (CVPR), 2016*.

[49] J. Deng, W. Dong, R. Socher, L.-J. Li, K. Li, and L. Fei-Fei, "Imagenet: A large-scale hierarchical image database," in *2009 IEEE Conference on Computer Vision and Pattern Recognition, 2009*, pp. 248–255.

[50] D. P. Kingma and J. Ba, "Adam: A method for stochastic optimization," in *Proceedings of 3rd International Conference on Learning Representations, 2015*.

[51] J. Long, E. Shelhamer, and T. Darrell, "Fully convolutional networks for semantic segmentation," in *Proceedings of the IEEE/CVF Conference on Computer Vision and Pattern Recognition (CVPR), 2015*.

[52] A. Paszke, S. Gross, F. Massa, A. Lerer, J. Bradbury, G. Chanan, T. Killeen, Z. Lin, N. Gimelshein, L. Antiga, A. Desmaison, A. Kopf, E. Yang, Z. DeVito, M. Raison, A. Tejani, S. Chilamkurthy, B. Steiner, L. Fang, J. Bai, and S. Chintala, "Pytorch: An imperative style, high-performance deep learning library," in *Advances in Neural Information Processing Systems, 2019*.

[53] L.-C. Chen, G. Papandreou, I. Kokkinos, K. Murphy, and A. L. Yuille, "Deeplab: Semantic image segmentation with deep convolutional nets, atrous convolution, and fully connected crfs," *IEEE Transactions on Pattern Analysis and Machine Intelligence*, vol. 40, no. 4, pp. 834–848, 2018.

[54] K. He, X. Zhang, S. Ren, and J. Sun, "Deep residual learning for image recognition," in *2016 IEEE Conference on Computer Vision and Pattern Recognition (CVPR), 2016*.

[55] O. Russakovsky, J. Deng, H. Su, J. Krause, S. Satheesh, S. Ma, Z. Huang, A. Karpathy, A. Khosla, M. Bernstein, A. C. Berg, and L. Fei-Fei, "ImageNet Large Scale Visual Recognition Challenge," *International Journal of Computer Vision (IJCV), 2015*.